Structural and Magnetic Studies of a Zigzag Chain Copper(II) Complex and a Dipolar Spin-coupled Copper(II) Dimer with the Versatile Ligand 5-[(2-carboxyphenyl)azo]-1,3-Dimethylbarbituric Acid†

Enrique Colacio,*[a] José Ruiz,[a] José M. Moreno,[a] Raikko Kivekäs,[b] Markku R. Sundberg,[b] José M. Dominguez-Vera[c] and Jean P. Laurent[c]

[a] *Departamento de Química Inorgánica, Facultad de Ciencias, Universidad de Granada, 18071 Granada, Spain*

[b] *Divison of Inorganic Chemistry, Department of Chemistry, University of Helsinki, Vuorikatu 20, SF-00100, Helsinki, Finland*

[c] *Laboratoire de Chimie de Coordination du CNRS, 205 route de Narbonne, 31077 Toulouse Cedex, France*

On treating H_2L {5-[(2-carboxyphenyl)azo]-1,3-dimethylbarbituric acid} with $Cu(NO_3)_2 \cdot 3H_2O$ in ethanol–water (4:1) the tetranuclear complex $[\{CuL(H_2O)\}_4]$ **1** is obtained. When **1** is dissolved in pyridine(py)–ethanol (1:1) the complex $[\{CuL(py) \cdot 3H_2O\}_n]$ **2** is isolated. Both complexes in pyridine solution yield $[CuL(py)_2]$ **3**. A magnetic study of **1** points to a ferromagnetic ground state ($S_T = 2$). The structures of **2** and **3** have been determined by X-ray crystallographic methods. The structure of **2** consists of infinite zigzag chains running along the *b* axis, in which copper ions are sequentially bridged by the barbituric ring. The copper presents a distorted square-pyramidal environment. In the basal plane, four bonds are formed with the ligand and the molecule of pyridine, while the apical position is occupied by an oxygen atom belonging to the barbituric ring of an adjacent fragment; the ligand then acts in a tetradentate fashion. The copper–copper intrachain distance is 6.322(3) Å. The structure of **3** consists of discrete $[CuL(py)_2]$ molecules in which the ligand acts in a tridentate fashion. The copper co-ordination is distorted square-pyramidal. The complex packs in the crystal lattice as symmetry-related pairs of molecules, with a Cu···Cu separation of 5.410(3) Å. From magnetic susceptibility measurements, complex **2** is found to exhibit ferromagnetic intrachain interactions with an exchange coupling of $J/2k = 1.7$, whereas a Curie–Weiss law is observed for **3**. Even though **3** lacks any close contact between molecules which may be regarded as bonding interactions, the polycrystalline EPR spectrum at 90 K exhibits a half-field signal, which is indicative of a spin-coupling process.

Although numerous examples exist of well structurally characterized *syn–anti* carboxylate bridged copper(II) complexes only a few of them so far have been studied magnetically.[1–9] These were characterized by feeble magnetic interactions that can be either ferromagnetic with *J* values ranging from 0.5 to 6.9 cm^{-1} or, in two instances, antiferromagnetic with $|J|$ values of 1.0 and 3.0 cm^{-1}.[5,6]

Generally, the *syn–anti* configuration favours the formation of either chain or layer compounds. Nevertheless, when the carboxylate group is incorporated into a polydentate ligand it is forced to adopt the *syn–anti* configuration and a great variety of structural and magnetic characteristics might be obtained. Thus, with the ligand H_2L^1 [H_2L^1 = 6-amino-1,3-dimethyl-5-(2′-carboxyphenyl)azouracil] we succeeded in obtaining a quasi-tetrahedral tetranuclear complex, having four bridging carboxylate groups in the *syn–anti* configuration.[8] Within this framework and following our current study on multiatom-bridged exchange-coupled systems,[8,9] we report in this paper on the magnetochemical studies of a presumably tetranuclear complex, formulated as $[\{CuL(H_2O)\}_4]$ **1**, with the ligand H_2L {H_2L = 5-[2′-carboxyphenyl)azo]-1,3-dimethylbarbituric acid}, which is closely related to the aforementioned H_2L^1 ligand. Likewise, in this work we report the structural and magnetic properties of the complexes $[\{CuL(py) \cdot 3H_2O\}_n]$ **2** and $[CuL(py)_2]$ **3**, which were obtained from $[\{CuL(H_2O)\}_4]$ in ethanol–pyridine and pyridine, respectively. Complex **2** containing pyrimidine bridges between copper(II) ions is one of the few examples of multiatom-bridged ferromagnetically coupled copper(II) complexes. Interestingly, complex **3** is a new example of a dipolar spin-coupled copper dimer.

Experimental

Preparation of the Compounds.—The ligand H_2L was prepared according to the method described previously.[10]

$[\{CuL(H_2O)\}_4]$ **1**. This complex was prepared by adding copper(II) nitrate trihydrate (0.242 g, 1 mmol) to a stirred suspension of freshly prepared H_2L (0.304 g, 1 mmol) in ethanol–water (50 cm^3, 4:1) at room temperature. After 10 min, a green powder precipitated which was filtered off, washed with ethanol and air-dried (Found: C, 40.6; H, 3.1; Cu, 16.8; N, 14.8. $C_{52}H_{48}Cu_4N_{16}O_{24}$ requires C, 40.7; H, 3.1; Cu, 16.6; N, 14.6%); IR (KBr, cm^{-1}) 1719 {ν[C(2)=O]}, 1645 {ν[C(6)=O]}, 1610 [$\nu_{asym}(CO_2)$], 1390 [$\nu_{sym}(CO_2)$] and 1380 [ν(N=N)]. Repeated attempts to obtain suitable crystals for structure determination have not been successful so far.

† *Supplementary data available* (No. SUP 56911, 2 pp.): EPR spectra. See Instructions for Authors, *J. Chem. Soc., Dalton Trans.*, 1993, Issue 1, pp. xxiii–xxviii.

Non-SI unit employed: G = 10^{-4} T.

Table 1 Fractional atomic coordinates for $[\{CuL(py)\cdot 3H_2O\}_n]$ **2**

Atom	*x*	*y*	*z*
Cu	0.678 15(5)	0.154 90(10)	0.120 06(4)
O(2)	0.467 0(3)	0.113 2(6)	0.387 3(2)
O(4)	0.594 7(2)	0.192 0(6)	0.187 8(2)
O(6)	0.759 2(2)	−0.035 4(6)	0.395 6(2)
O(16)	0.740 6(2)	0.026 0(7)	0.054 7(2)
O(17)	0.854 5(3)	−0.069 3(7)	0.003 6(2)
N(1)	0.615 6(3)	0.053 6(7)	0.393 3(2)
N(3)	0.533 4(3)	0.160 3(7)	0.288 3(2)
N(7)	0.766 9(3)	0.076 7(7)	0.261 7(2)
N(8)	0.773 2(3)	0.106 8(6)	0.196 2(2)
N(18)	0.583 0(3)	0.215 5(7)	0.040 9(2)
C(1)	0.617 2(5)	0.004 0(1)	0.468 0(3)
C(2)	0.533 8(4)	0.109 3(8)	0.358 0(3)
C(3)	0.446 7(4)	0.218 0(10)	0.250 0(4)
C(4)	0.605 7(3)	0.148 7(8)	0.251 3(3)
C(5)	0.688 2(3)	0.086 6(8)	0.288 3(3)
C(6)	0.692 9(3)	0.030 7(8)	0.361 3(3)
C(9)	0.864 6(3)	0.113 7(8)	0.181 6(3)
C(10)	0.888 4(3)	0.065 3(8)	0.115 6(3)
C(11)	0.978 8(4)	0.079 0(10)	0.105 2(3)
C(12)	1.042 5(4)	0.143 0(10)	0.157 6(3)
C(13)	1.017 7(4)	0.195 0(10)	0.221 5(3)
C(14)	0.929 6(4)	0.180 0(9)	0.233 7(3)
C(15)	0.824 6(4)	0.001 1(9)	0.054 3(3)
C(19)	0.495 4(4)	0.207 0(10)	0.046 3(3)
C(20)	0.431 0(4)	0.257 0(10)	−0.008 0(4)
C(21)	0.457 6(5)	0.317 0(10)	−0.069 2(4)
C(22)	0.548 1(5)	0.323 0(10)	−0.076 5(3)
C(23)	0.608 1(4)	0.271 0(10)	−0.020 4(3)
O(24)	0.724 0(3)	−0.163 9(8)	−0.106 8(2)
O(25)	0.282 1(3)	−0.130 1(8)	0.201 2(3)
O(26)	0.277 6(3)	0.013 6(8)	0.341 9(3)

Table 2 Fractional atomic coordinates for $[CuL(py)_2]$ **3**

Atom	*x*	*y*	*z*
Cu	0.888 1(2)	0.585 19(8)	0.366 7(3)
O(4)	0.998(1)	0.570 4(4)	0.599(1)
N(8)	1.038(1)	0.630 9(4)	0.352(2)
O(6)	1.354(1)	0.691 7(4)	0.723(1)
O(16)	0.810(1)	0.578 4(5)	0.136(1)
N(3)	1.163(1)	0.577 7(5)	0.855(2)
O(2)	1.328(1)	0.585 8(5)	1.113(2)
N(24)	0.757(1)	0.646 4(5)	0.424(2)
N(7)	1.140(1)	0.647 9(4)	0.478(2)
N(18)	0.749(1)	0.530 1(5)	0.379(2)
C(14)	0.931(2)	0.641 7(6)	0.044(2)
N(1)	1.349(1)	0.637 8(5)	0.917(2)
C(6)	1.294(2)	0.656 9(6)	0.756(2)
C(5)	1.175(2)	0.631 3(6)	0.635(2)
C(19)	0.630(2)	0.521 9(7)	0.244(2)
C(9)	1.035(2)	0.655 2(6)	0.198(2)
C(4)	1.105(2)	0.593 3(6)	0.693(2)
C(21)	0.565(2)	0.454 7(6)	0.378(2)
C(10)	1.131(2)	0.692 2(6)	0.207(2)
C(11)	1.128(2)	0.716 0(6)	0.062(2)
O(17)	0.753(2)	0.593 0(6)	−0.127(2)
C(13)	0.928(2)	0.666 3(6)	−0.101(2)
C(29)	0.778(2)	0.692 8(8)	0.402(2)
C(12)	1.025(2)	0.703 6(6)	−0.094(2)
C(25)	0.645(2)	0.634 5(6)	0.478(2)
C(23)	0.778(2)	0.500 6(7)	0.517(2)
C(3)	1.092(2)	0.536 3(6)	0.916(2)
C(15)	0.823(2)	0.600 3(6)	0.018(2)
C(1)	1.476(2)	0.659 8(6)	1.042(2)
C(22)	0.684(2)	0.462 4(6)	0.515(2)
C(20)	0.531(2)	0.484 5(7)	0.239(2)
C(26)	0.548(2)	0.667 1(7)	0.504(2)
C(2)	1.282(2)	0.600 5(6)	0.967(2)
C(27)	0.574(2)	0.715 4(7)	0.479(2)
C(28)	0.686(2)	0.728 1(8)	0.426(2)

$[\{CuL(py)\cdot 3H_2O\}_n]$ **2**. The complex can be prepared using two different procedures: (*i*) to a solution of freshly prepared H_2L (0.304 g, 1 mmol) in pyridine–ethanol (50 cm^3, 1:1) was added copper(II) nitrate trihydrate (0.242 g, 1 mmol) as a solid. The solid dissolved quickly upon stirring, to give a deep green solution. Slow evaporation of the solution gave green needle shaped crystals suitable for X-ray diffraction study (Found: C, 43.4; H, 3.8; Cu, 12.6; N, 14.4. $C_{18}H_{21}CuN_5O_8$ requires C, 43.3; H, 4.2; Cu, 12.7; N, 14.0%); IR (KBr, cm^{-1}) 1705 {ν[C(2)=O]}, 1635 {ν[C(6)=O]}, 1620 [$\nu_{asym}(CO_2)$], 1390 [$\nu_{sym}(CO_2)$], 1380 [ν(N=N)] and 700 [δ(C–H)]. (*ii*) Complex **2** can also be obtained by dissolution of **1** (0.384 g, 1 mmol) in pyridine–ethanol (50 cm^3, 1:1).

$[CuL(py)_2]$ **3**. This compound was prepared according to two different procedures: (*i*) copper(II) nitrate trihydrate (0.242 g, 1 mmol) was added to a stirred solution of freshly prepared H_2L (0.304 g, 1 mmol) in pyridine (25 cm^3). When the resulting clear solution was allowed to stand for two weeks at room temperature, poor quality black crystals were formed, which were collected by filtration (Found: C, 52.7; H, 3.9; Cu, 12.0; N, 15.8. $C_{23}H_{20}CuN_6O_5$ requires C, 52.7; H, 3.8; Cu, 12.1; N, 16.0%); IR (KBr, cm^{-1}) 1710 {ν[C(2)=O]}, 1659 {ν[C(6)=O]}, 1620 [$\nu_{asym}(CO_2)$], 1395 [$\nu_{sym}(CO_2)$], 1380 [ν(N=N)] and 700 [δ(C–H)]. (*ii*) This compound can also be obtained by dissolving $[\{CuL(H_2O)\}_4]$ (1.53 g, 1 mmol) in pyridine (25 cm^3).

Physical Measurements.—Microanalyses of C, H and N, infrared and EPR spectra as well as the magnetic susceptibility data were obtained as already described.[8] Copper was determined thermogravimetrically, as CuO, using a Mettler TG-50 thermobalance.

X-Ray Data Collection and Structure Determination.—Single-crystal data collections were performed at 293 K with a Siemens R3m/V diffractometer using graphite monochromatized Cu-Kα (λ = 1.5418 Å) and Mo-Kα (λ = 0.710 69 Å) radiation, for **2** and **3**, respectively. Prismatic deep green and black crystals were used with dimensions 0.18 × 0.22 × 0.25 and 0.21 × 0.15 × 0.10 mm for **2** and **3**, respectively. Complex **2** crystallizes in the monoclinic system, space group $P2_1/n$, with a = 15.070(8), b = 7.230(4), c = 19.165(10) Å, β = 96.86(1)°, U = 2072(2) $Å^3$, Z = 4, D_c = 1.60 g cm^{-3}, $F(000)$ = 1028 and μ(Cu-Kα) = 1.96 mm^{-1}. Complex **3** crystallizes in the monoclinic system, space group $P2_1/c$, a = 9.927(2), b = 27.941(6), c = 8.524(2) Å, β = 110.23(3)°, U = 2218.5(8) $Å^3$, Z = 4, D_c = 1.57 g cm^{-3}, $F(000)$ = 1076, μ(Mo-Kα) = 1.033 mm^{-1}.

It must be noted that for **3** several crystals were tested, but all of them displayed only very moderate diffraction power, obviously due to disorder of the structure. Numerous attempts were also made to obtain better crystals using gelled and salting-out methods, but there was no improvement in the crystal quality.

The unit-cell parameters were calculated by least-squares refinement of 25 well centred reflections in the range 3 < 2θ < 60° and 5 < 2θ < 25°, for **2** and **3**, respectively. The data were collected by ω–2θ scan mode (3 < 2θ < 125° for **2** and 3 < 2θ < 62° for **3**). Intensities of three check reflections measured after every 120 minutes showed only statistical variation. A total of 2376 and 1211 reflections were considered as observed with $F > 4\sigma(F_o)$ and $F > 5\sigma(F_o)$, for **2** and **3**, respectively. The data were corrected for Lorentz and polarization effects and, in the case of **3**, for absorption.

For **2**, the direct methods of the SHELXS program[11] were used to find the positions of heavy atoms. Subsequent Fourier synthesis and least-squares refinement using the XTAL[12] program allowed the location of all atoms. In the final cycles the non-hydrogen atoms were refined anisotropically and the

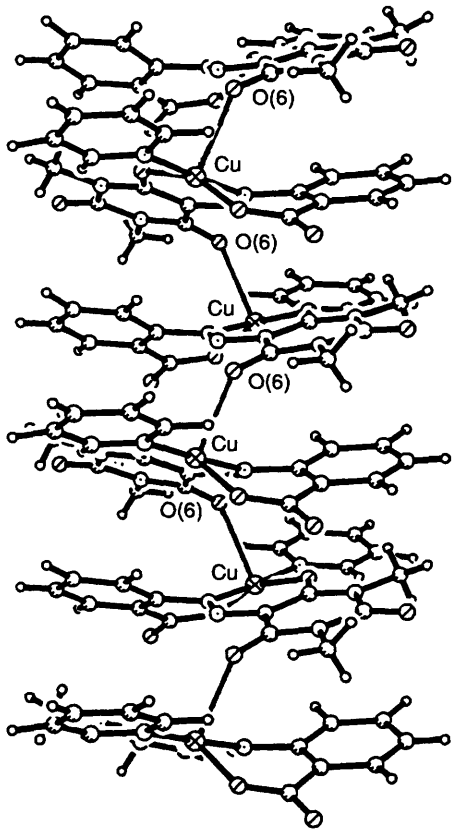

Fig. 1 A perspective view of the linear chain of complex **2** along the *b* axis

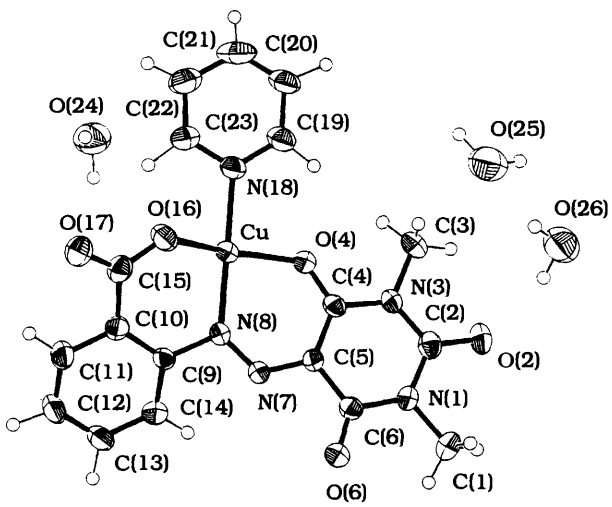

Fig. 2 A perspective view of the mononuclear fragment of complex **2**

hydrogen atoms of the ligand with isotropic thermal parameters. The hydrogen atoms of the water molecules were given fixed isotropic thermal parameters (U = 0.050 Å^2) and were not refined.

For **3**, the structure was solved by direct methods and subsequent Fourier syntheses using the SHELXTL PLUS program.[13] The final refinement was performed with the programs of the XTAL package.[12] Copper and the atoms co-ordinated to it were refined anisotropically and the remaining non-hydrogen atoms isotropically. In both cases, neutral-atomic scattering and dispersion factors were those included in the program packages.

The function minimized was $\Sigma w(\Delta F)^2$ $[1/w = \sigma^2(F_o)]$, resulting in final $R = \Sigma||F_o| - |F_c||/\Sigma|F_o|$ values of 0.040 and 0.066 and $R' = [\Sigma w(|F_o| - |F_c|)^2/\Sigma w|F_o|^2]^{\frac{1}{2}}$ values of 0.048 and 0.073 for **2** and **3**, respectively. Atomic coordinates for the non-hydrogen atoms are listed in Tables 1 and 2 for complexes **2** and **3** respectively.

Additional material available from the Cambridge Crystallographic Data Centre comprises H-atom coordinates, thermal parameters and remaining bond lengths and angles.

Table 3 Selected bond lengths (Å) and angles (°) for $[\{CuL(py)\cdot 3H_2O\}_n]$ **2***

Cu–O(4)	1.941(5)	Cu–O(6^I)	2.462(4)
Cu–N(8)	2.000(7)	C(15)–O(16)	1.279(7)
Cu–O(16)	1.866(6)	C(15)–O(17)	1.228(8)
Cu–N(18)	2.092(8)	N(7)–N(8)	1.289(6)
O(4)–Cu–O(6)	104.2(2)	O(6)–Cu–N(18)	87.7(2)
O(4)–Cu–O(16)	157.8(2)	O(16)–Cu–N(8)	91.6(2)
O(4)–Cu–N(8)	90.1(2)	O(16)–Cu–N(18)	88.5(2)
O(4)–Cu–N(18)	90.8(2)	N(8)–Cu–N(18)	177.4(3)
O(6)–Cu–O(16)	98.0(2)	O(16)–C(15)–O(17)	121.3(5)
O(6)–Cu–N(8)	89.7(2)		

Relevant hydrogen bond distances (Å)

O(24)···O(26^{II})	2.863(8)	O(17)···O(24)	2.796(6)
O(24)···O(25^{IV})	2.786(8)	O(25)···O(26^{III})	2.819(8)
O(26)···O(2)	2.971(6)	O(25)···O(26)	2.897(7)

* Symmetry operations: I $\frac{1}{2} - x, \frac{1}{2} + y, \frac{1}{2} - z$; II $-\frac{1}{2} + x, \frac{1}{2} - y, \frac{1}{2} + z$; III $-\frac{1}{2} + x, \frac{3}{2} - y, \frac{1}{2} + z$; IV $2 - x, 1 - y, 1 - z$.

Results and Discussion

On treating H_2L with $Cu(NO_3)_2\cdot 3H_2O$ in ethanol–water (4:1), the complex with empirical formula $[\{CuL(H_2O)\}_4]$ **1** is obtained. When **1** is dissolved in pyridine–ethanol (1:1) the complex $[\{CuL(py)\cdot 3H_2O\}_n]$ **2** is isolated. Either **1** or **2** in pyridine solution yields the complex $[CuL(py)_2]$ **3**.

Because all of these complexes exhibit powder EPR spectra suggestive of magnetically coupled copper(II) centres, we have performed a detailed characterization of them, including the crystal structure determination of the complexes **2** and **3**.

Crystal Structure of **2**.—The structure consists of infinite zig-zag chains running along the crystallographic *b* axis (Fig. 1), in which copper(II) ions are bridged sequentially by the barbituric ring with a Cu ··· Cu distance of 6.322(3) Å. A perspective view of the mononuclear fragment together with the atomic labelling scheme is given in Fig. 2. Selected bond distances and angles are listed in Table 3.

The environment of each copper ion is (4 + 1). Four short bonds of *ca.* 2.0 Å are formed with the O(4), N(8) and O(16) atoms from the double-deprotonated ligand and N(18) atom from the pyridine molecule. The O(6^I) oxygen atom belonging to the barbituric moiety of an adjacent symmetry related fragment (I $\frac{1}{2} - x, \frac{1}{2} + y, \frac{1}{2} - z$) is co-ordinated in an axial position at a longer distance, 2.462(4) Å, giving rise to the chain. The bond lengths in the co-ordination polyhedron have normal values.[8,9] It must be pointed out that the co-ordination of the O(6^I) oxygen atom of the pyrimidine moiety to the copper atom of a neighbouring unit is quite unusual. This has only been previously observed in the complexes $[\{Cu_4L^1{}_3(HL^1)(NO_3)(H_2O)\cdot 2H_2O\}_n]$[8] and $[\{CuL(Him)\}_2]$[14] (Him = imidazole), with Cu–O(6^I) bond distances of 2.31(2) and 2.651(3) Å, respectively. The (4 + 1) co-ordination mode is compatible with two idealized geometries: square pyramidal and trigonal bipyramidal. The procedure proposed by Muetterties and Guggenberg[15] locates the co-ordination polyhedron at 36.4% towards D_{3h} of the $C_{4v} \longleftrightarrow D_{3h}$ deformation pathway. In a square-pyramidal description, the equatorial ligands are not coplanar but pair-wise distorted, so that N(8) and N(18) are lifted 0.202(7) and 0.244(8) Å above the mean basal plane while

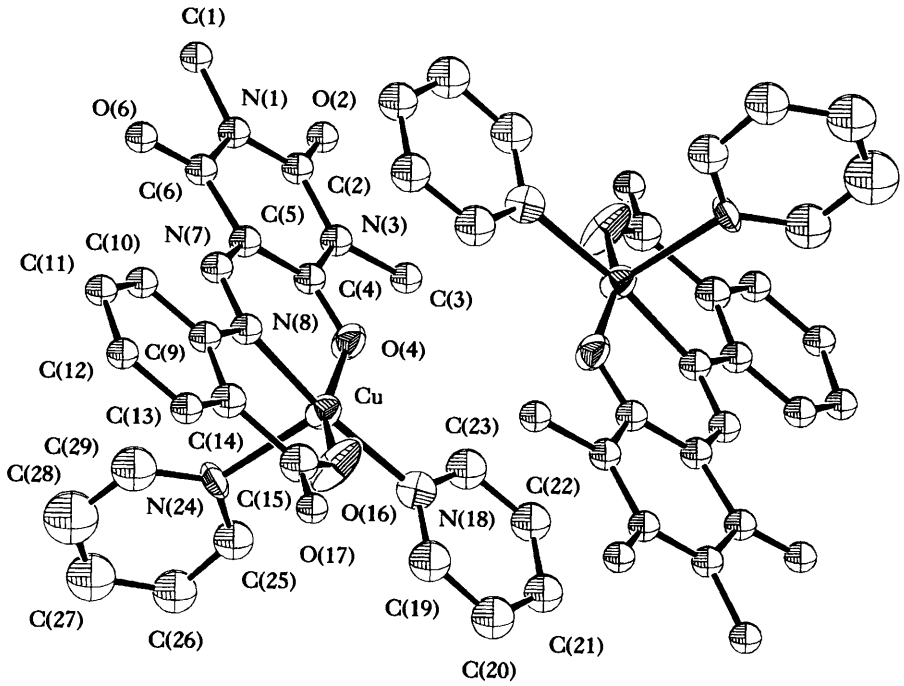

Fig. 3 A perspective view of complex **3**

Table 4 Selected bond lengths (Å) and angles (°) for $[CuL(py)_2]$ **3**

Cu–O(4)	1.944(9)	N(7)–N(8)	1.283(14)
Cu–N(8)	1.993(12)	C(14)–C(15)	1.542(21)
Cu–O(16)	1.857(10)	C(15)–O(16)	1.222(21)
Cu–N(18)	2.097(13)	C(15)–O(17)	1.207(19)
Cu–N(24)	2.303(13)		
O(4)–Cu–N(8)	91.8(4)	N(8)–Cu–N(24)	92.6(5)
O(4)–Cu–O(16)	159.5(5)	O(16)–Cu–N(18)	86.5(5)
O(4)–Cu–N(18)	86.6(4)	O(16)–Cu–N(24)	104.1(5)
O(4)–Cu–N(24)	95.8(4)	N(18)–Cu–N(24)	95.9(5)
N(8)–Cu–O(16)	92.6(5)	O(16)–C(15)–O(17)	125.0(15)
N(8)–Cu–N(18)	172.6(5)		

O(4) and O(16) are located 0.163(7) and 0.215(8) Å below the plane. As usual, the copper(II) ion is lifted by 0.177(3) Å from the mean plane towards the apical $O(6^I)$ atom.

The tridentate behaviour of the ligand results in the formation of two six-membered rings having in common the Cu–N(8) bond. Bonds lengths and angles in the ligand do not significantly differ from those found in the complexes $[\{CuL(H_2O)\}_n]$[9] and $[\{CuL(Him)\}_2]$.[14] In the pyridine ligand, the C–C and C–N bond lengths and angles are within the expected range. The pyrimidine, pyridine and phenyl rings are almost planar with deviations from the least-squares plane less than 0.083 Å. The pyrimidine and phenyl rings in the neighbouring units are almost parallel. The shortest intermolecular pyrimidine–phenyl contact distance C(9) · · · $C(2^I)$ of 3.217(8) Å ($I\ \frac{1}{2} - x, \frac{1}{2} + y, \frac{1}{2} - z$) is less than the sum of the van der Waals radii, indicating that steric crowding exists in the structure.

Neighbouring chains are interconnected by a hydrogen bonding system involving the oxygen atoms O(2) and O(17) and three water molecules, with the shortest interchain Cu · · · Cu distance being 7.008(3) Å. Relevant hydrogen-bonding distances are given in Table 3.

Crystal Structure of **3**.—A perspective view of $[CuL(py)_2]$ together with the atomic numbering schemes is given in Fig. 3. Selected bond distances and angles are listed in Table 4. The structure consists of discrete $[CuL(py)_2]$ molecules, in which the copper atom adopts a (4 + 1) co-ordination mode. As in **2**, the double-deprotonated ligand affords three co-ordination sites, namely the N(8) nitrogen atom of the azo group and the O(4) and O(16) oxygen atoms belonging to the deprotonated hydroxy and carboxylate groups, respectively. The two remaining co-ordination sites are occupied by the nitrogen atoms of the pyridine molecules. Consideration of the angles around the copper(II) ion shows that the conformation of the CuN_3O_2 chromophore is not far removed from ideal square-pyramidal geometry. According to the Muetterties procedure, the shape of the co-ordination polyhedron lies on the $C_{4v} \longleftrightarrow D_{3h}$ deformation pathway, with a C_{4v} character of 75%.

In the square-pyramidal description, the basal plane is defined by O(4), N(8), O(16) and N(18), whereas the apical position is occupied by N(24) from a pyridine molecule, in accordance with the relatively large Cu–N(24) distance of 2.30(1) Å. As found in **2**, pyrimidine, phenyl and pyridine rings are almost planar with deviation from the least-square planes less than 0.06 Å.

The equatorial pyridine ring is not coplanar with the tridentate ligand but twisted by an angle of 8.2° with respect the pyrimidine ring, whilst the mean planes of the pyridine ligands make an angle of 102.6° to each other. The C(23) · · · O(4) and C(19) · · · O(16) contact distances are both less than 3.2 Å, the respective sum of the van der Waals radii, indicating that steric crowding exists in the structure.

The molecules are packed in symmetry-related basal plane to basal plane pairs with a Cu · · · Cu^I ($I\ -x, -y, -z$) separation of 5.410(3) Å. Within each pair of symmetry-related molecules, the pyrimidine ring of one molecule is over the equatorial pyridine ring of the other molecule and the pyridine ring over the pyrimidine ring. An interesting feature of the structure is the lack of any close contacts between molecules which might be expected to engage in bonding interactions. The shortest intermolecular contact distance is 3.37(2) Å between the C(23) pyridine atom of a molecule and the $O(4^I)$ pyrimidine atom of a symmetry-related molecule. In view of this, crystal packing forces, presumably, of an attractive π type, may be responsible for the pairwise arrangement of the molecules. Such an arrangement has also been observed in the dipolar spin-

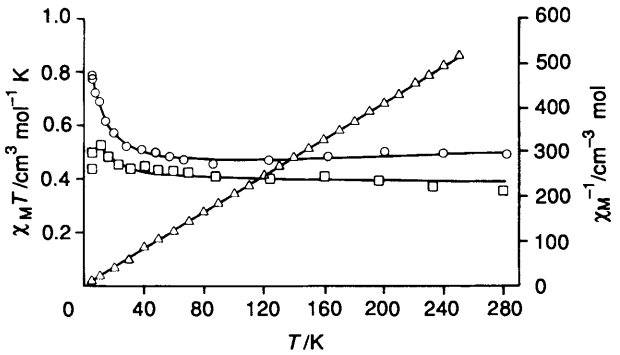

Fig. 4 Plot of $\chi_M T$, for **1** (○) and **2** (□), and of χ_M^{-1} for **3** (△) *vs.* T. The solid lines were generated from the best-fit magnetic parameters. The solid line for **1** was calculated from equation (1) assuming T_d symmetry

coupled dimer $[\{CuL^2(dbm)\}_2]$ {HL^2 = 1,3-bis[(5-methyl-2-pyridyl)imino]isoindoline, dbm = dibenzoylmethane}.[16]

Spectroscopic Data.—The IR spectrum of **1** is very similar to that of $[\{Cu_4L^1{}_3(HL^1)(NO_3)(H_2O)\}_n]\cdot 2H_2O$,[8] a Cu_4 cluster with *syn–anti* carboxylate bridges between each two copper atoms, except for the lack of absorptions corresponding to the nitrate ion, suggesting that the co-ordination mode of the ligand is analogous in both complexes. As in **2** and **3**, which are obtained from **1**, the two remaining co-ordination sites of the ligand would be the N(8) nitrogen atom of the azo group and the O(4) exocyclic oxygen atom of the pyrimidine ring, giving rise to a $CuNO_4$ co-ordination polyhedron.

The IR spectra of **2** and **3** exhibit features characteristic of the co-ordination modes of L^{2-} and pyridine. Interestingly, in **2** the C(6)=O is shifted to lower frequencies by *ca.* 25 cm^{-1} with respect to its position in **3**, which might be due to the co-ordination of the O(6) oxygen atom to the copper(II) ion, in agreement with the crystal structure of **2**.

The reflectance spectrum of **1** shows an absorption maximum at 16 000 cm^{-1}, which is consistent with a pseudo-square-pyramidal geometry for the copper ion rather than a trigonal-bipyramidal geometry.[17] The spectra observed for **2** (16 000 cm^{-1}) and **3** (16 000 and 10 500 cm^{-1}) are also consistent with a square-based pyramidal geometry for the copper ion, in good agreement with their crystal structures.

Magnetic Data.—For **1**, the temperature dependence of χ^{-1} from 281.4 to 4.6 K is well fitted to a Curie–Weiss law with C = 0.49 cm^3 K mol^{-1} and θ = 0.83 K. From the positive value of θ, it can be estimated that the complex displays an overall ferromagnetic behaviour. This is also apparent from a consideration of the thermal variation of the product $\chi_M T$, which is displayed in Fig. 4. From 281 to *ca.* 100 K, $\chi_M T$ remains practically constant and equal to 0.49 cm^3 K mol^{-1}. On further lowering of the temperature, $\chi_M T$ increases, yielding an extrapolated value of *ca.* 0.84 cm^3 K mol^{-1} at 0 K. The value would correspond to a state characterized by a spin of 2 with a g value of 2.12. The temperature dependence of the magnetic susceptibility is comparable to that of the tetranuclear complex $[\{Cu_4L^1{}_3(HL^1)(NO_3)(H_2O)\}_n]\cdot 2H_2O$.[8]

The lack of molecular structure determination for **1** does not allow, initially, the choice of a suitable model to analyse the magnetic data. At this point, it must be noted that, even though **1** has the same empirical formula as $[\{CuL(H_2O)\}_n]$,[9] a *syn–anti* carboxylate-bridged helix-like chain compound also exhibiting ferromagnetic intrachain interaction, significant differences exist between their ligand-field and EPR spectra. Thus, the maximum observed in the reflectance spectrum of $[\{CuL(H_2O)\}_n]$ at 14 300 cm^{-1} lies to significantly lower energy than that of **1**. The room-temperature EPR spectrum of a powdered sample of **1** exhibits an intense and quasi-isotropic resonance at g = 2.12 and a weaker signal at 4.12. Lowering the temperature from 300 to 5 K does not alter the overall appearance of the spectrum but increases its intensity. The spectrum of $[\{CuL(H_2O)\}_n]$ is quite different to that of **1**, exhibiting two main features attributable to parallel (g = 2.23) and perpendicular (g = 2.05) components of an axially symmetrical spectrum with several small signals discernible between these two features. Although the spectroscopic data suggest that **1** and $[\{CuL(H_2O)\}_n]$ have different structures, a chain structure other than that observed for the latter could not be wholly discarded for **1**.

On the other hand, it must be pointed out that the EPR spectral features of **1** are similar to those observed for the tetranuclear complex $[\{Cu_4L^1{}_3(HL^1)(NO_3)(H_2O)\}_n]\cdot 2H_2O$[8] (an intense and quasi-isotropic resonance at g = 2.12 and a weaker signal at 4.29). To the best of our knowledge, the EPR signals attributable to transitions within the quintet state have seldom been observed for tetranuclear complexes,[18–21] and the experimental data for both $[\{Cu_4L^1{}_3(HL^1)(NO_3)(H_2O)\}_n]\cdot 2H_2O$ and **1** seem to be in accord with a triplet state. In view of the close similarity between the EPR spectra and magnetic behaviour for these two compounds, a tetranuclear structure containing *syn–anti* carboxylate bridges between copper ions, like that of $[\{Cu_4L^1{}_3(HL^1)(NO_3)(H_2O)\}_n]\cdot 2H_2O$, could be proposed tentatively for **1**. This would represent one of the few examples of tetranuclear copper(II) compounds containing only polyatomic bridges.[8,22] The most commonly observed types of Cu_4 clusters are those containing either the Cu_4O_4 core (cubane-like complexes), with bridging alkoxide oxygen atoms, or the $[Cu_4OX_{10-n}L_n]^{n-4}$ core (X = halide, L = neutral ligand) with both μ_4-bridging oxygens and μ-bridging halides between the copper ions.[22] In both types of tetranuclear copper(II) compounds monoatomic bridges interconnect the metal ions.

In light of the above discussion, we have fitted the magnetic data to the theoretical expressions of χ_M for various reasonable models of Cu_4 clusters, including the idealized symmetries T_d, D_{2d} and D_{4h}. A correction for a small amount of paramagnetic impurity ($S = \frac{1}{2}$) was also taken into account by inserting a Curie law expression into equation (1) where p is the amount of

$$\chi_{calc} = \left[\frac{C}{T} f(u,v)\right](1 - p) + pC/T + \text{t.i.p.} \qquad (1)$$

paramagnetic impurity, $C = Ng^2\beta^2/4k$, t.i.p. = 60×10^{-6} cm^3 mol^{-1} for each copper (where t.i.p. = temperature independent paramagnetism), $f(u,v)$ is as given in the literature with $u = J_{i,j}kT$ (T_d),[23] $u = J_{1,3}/kT$ and $v = J_{1,2}/kT$ (D_{2d})[24] and $u = J_{cis}/kT$ and $v = J_{trans}/kT$ (D_{4h}).[23]

The experimental values of χ_M have been fitted by these equations by treating g, p and the exchange coupling constants as adjustable parameters. Except for D_{2d} symmetry which does not show any reliable fit, the parameters resulting from the fits of the magnetic data are: $J_{i,j}$ = 6.7 cm^{-1}, g = 2.10, p = 0, R = 3×10^{-4} for T_d and J_{cis} = 8.5 cm^{-1}, J_{trans} = 1.7 cm^{-1}, g = 2.12, R = 4×10^{-4} for D_{4h} geometry; $R = \Sigma_i[(\chi_i^{obs} - \chi_i^{calc})^2(\chi_i^{obs})^2]$.

On the other hand, we have also fitted the magnetic data to Baker's expression[25] [equation (2)] for a $S = \frac{1}{2}$ ferromagnetic

$$\chi = \left[\frac{N\langle g\rangle^2\beta^2}{4kT}\right]\left[\frac{1 + Ax + Bx^2 + Cx^3 + Dx^4 + Ex^5}{1 + A'x + B'x^2 + C'x^3 + D'x^4}\right]^{\frac{4}{3}} \qquad (2)$$

chain, where $x = J/2kT$, A = 5.797 991 6, B = 16.902 653, C = 29.376 885, D = 29.832 956, E = 14.036 918, A' = 2.797 991 6, B' = 7.008 678 0, C' = 8.653 864 4 and D' = 4.574 311 4. From the best fit the parameters g = 2.0 and $J/2k$ = 2.2 ($R = 2 \times 10^{-2}$) were obtained.

The relative difference in the fits between the two Cu_4 geometries (T_d and D_{4h}) was small, although the fits were both considerably better than those for the chain model. These results seem to support the proposed tetranuclear structure for

1. Taking into account that in D_{4h} symmetry an important steric crowding would exist, it is reasonable to propose a pseudo-tetrahedral arrangement for copper(II) atoms in the Cu_4 cluster, like that observed for $[\{Cu_4L^1{}_3(HL^1)(NO_3)(H_2O)\}_n]\cdot 2H_2O$. Further studies are in progress to investigate the structure by using X-ray powder diffraction and/or single-crystal synchroton techniques.

Owing to the *syn–anti* conformation of the (Cu–O–C–O′–Cu′) bridges, the 2p orbitals of O and O′ belonging to the magnetic orbital centred on Cu and Cu′, respectively, are unfavourably oriented to give a strong overlap. This would cause a reduction of the antiferromagnetic contribution,[26] which would lead ultimately to the overall observed ferromagnetic behaviour. Although some other factors, such as the geometry around the copper atom and planarity of the Cu–O–C–O′–Cu′ fragment,[9] may be responsible for the lowering of the antiferromagnetic contribution, the conformation of the bridges must be the main factor leading to the overall ferromagnetic behaviour observed in the present case.

The temperature dependence of $\chi_M T$ for complex **2** is shown in Fig. 4. On lowering the temperature, the product $\chi_M T$ increases steadily from 0.39 cm^3 K mol^{-1} at 279 K, reaches a broad maximum of 0.54 cm^3 K mol^{-1} at 10 K and then slightly decreases upon cooling down to 0.44 cm^3 K mol^{-1} at 4.4 K. The results clearly indicate the operation of ferromagnetic coupling in this complex, as does the temperature dependence of χ_M^{-1}, which is well represented by a Curie–Weiss law with $C = 0.37$ cm^3 K mol^{-1} and $\theta = 3.90$ K ($g = 2.03$). The decrease of $\chi_M T$ at low temperature may be attributed to an interchain antiferromagnetic interaction.

In keeping with the chain structure, the quantitative analysis of the data may be performed using Baker's expression[25] which is based on the high-temperature Padé expansion technique. The best fit of the equation to the data was found with $J/2k = 1.70$ and $g = 2.05$ with $R = 2 \times 10^{-4}$. Attempts to improve the fit by taking into account interchain interactions *via* a mean field approximation[27] failed.

The presence of the definite, but weak, ferromagnetic coupling is consistent with the structure of **2**. From the structural data, a pathway for the observed spin coupling could be Cu(1)O(4)C(4)C(5)C(6)O(6)Cu(1′) [alternatively *via* N(8) and N(7)]. This pathway is extended and involves an axial position where the spin density is very weak (in a distorted square-planar geometry the unpaired electron is in a predominantly either $d_{x^2-y^2}$ or d_{xy} orbital). Because of this, a slight overlap of the magnetic orbitals centred on Cu(1) and Cu(1′) is expected. This would cause a reduction of the antiferromagnetic contribution[26] so that the ferromagnetic contribution becomes predominant.

At room temperature the X-band spectrum of a powdered sample appears axial ($g_{\|} = 2.19$ and $g_{\perp} = 2.08$), as expected for a copper(II) ion with either $d_{x^2-y^2}$ or d_{xy} ground state. Lowering the temperature to 5 K produces no effect on the shape and positions of the signals but increases its intensity slightly allowing the detection, at high gain, of a half-field $\Delta M_s = 2$ signal at 1635 G.

The polycrystalline X-band EPR spectrum of **3** at 90 K (Fig. S1, SUP 56911) shows the features characteristic of a dinuclear copper system, with resonances corresponding to $\Delta M_s = 1$ ($g_{\|} = 2.20$ and $g_{\perp} = 2.08$) and $\Delta M_s = 2$ ($H = 1654$ G). The intensity of the half-field signal decreases dramatically at ambient temperature. The signals are devoid of any hyperfine structure, which may be due to dipolar broadening effects. The axial spectrum with $g_{\|} > g_{\perp} > 2.0$ is consistent with the observed distorted square-pyramidal geometry for the complex.

Magnetic susceptibility data were collected in the temperature range 250–5 K and they are displayed in Fig. 4 as $\chi_M T$ *vs.* T. The product $\chi_M T$ remains practically constant down to 5 K indicating that $|J| < \approx 0.5$ cm^{-1}. The data obey the Curie–Weiss law with $C = 0.49$ cm^3 K mol^{-1} and $\theta = -0.11$ K. From the expression defining θ in terms of the molecular-field exchange parameter,[27] a value for zJ' of -0.15 cm^{-1} can be obtained where z is the number of nearest neighbours.

The results from the structural determination clearly indicate that there is no bridging atom or group of atoms through which a magnetic interaction may be mediated. In addition, the Cu · · · Cu separation within each dimer is too large for a direct overlap between copper orbitals. Because there is evidence from the EPR powder spectrum of the presence of magnetically coupled, yet apparently isolated, copper(II) atoms, it is reasonable to assume that the coupling is purely dipolar in nature. A similar pairwise dipolar coupling was also observed in the complex $[CuL^2(dbm)]$.[16]

Interestingly, in pyridine solution at 90 K, complexes **1** and **2** exhibit essentially superimposable EPR spectra, with signals attributable to an axial doublet spectrum ($g_{\|} = 2.26$ and $g_{\perp} = 2.07$) and two additional absorptions at 3500 and 3066 G, respectively. In addition, the half-field signal transition ($\Delta M_s = 2$) was observed at 4.12. The $g_{\|}$ component of the doublet spectrum shows a four-line hyperfine structure with $|A| = 158 \times 10^{-4}$ cm^{-1}, while five lines of superhyperfine structure with $|A| = 13 \times 10^{-4}$ cm^{-1} are observed on the perpendicular component. The observed spectral features seem to indicate that pyridine causes dissociation of both **1** and **2** into a mononuclear complex, giving rise to the doublet spectrum and a dinuclear species, both coexisting in solution. The separation between the two additional signals of 434 G (0.04 cm^{-1}) suggests the occurrence of significant zero-field splitting effects. Surprisingly, it appears that **3** dissolved in pyridine leads to a similar monomer–dimer equilibrium in solution as for **1** and **2**. When dimethyl sulfoxide (dmso) is used as solvent, the EPR spectra of **2** and **3** at 90 K (Fig. S1, SUP 56911) show a similar pattern comprising an axial doublet spectrum ($g_{\|} = 2.25$, $g_{\perp} = 2.05$ and $|A_{\|}| = 158 \times 10^{-4}$ cm^{-1} and a pair of zero-field split transitions at 3530 and 3036 G). The half-field ($\Delta M_s = 2$) transition appears as a seven-line hyperfine pattern at 1520 G, with an average hyperfine spacing of 77×10^{-4} cm^{-1}. The appearance of this pattern confirms the presence of a dinuclear complex in solution. Moreover, in the region 2410–2630 G, four poorly resolved copper hyperfine lines can be observed with an average spacing of 78×10^{-4} cm^{-1}. The other three lines of this seven-line pattern are obscured by the hyperfine lines of the doublet $g_{\|}$ signal. There should be another seven-line pattern resulting from the zero-field splitting at a much higher field position. However, none of the hyperfine components of the high-field seven-line pattern resulting from the zero-field splitting was located in the spectra. Finally, it should be noted that the copper hyperfine spacings of $\Delta M_s = 1$ and $\Delta M_s = 2$ signals for the dinuclear complex are almost half that of the mononuclear complex responsible for the axial doublet spectrum, as expected for an exchange-coupled copper(II) dimer.[28] It must be pointed out that no new spin-triplet signals are observed in the EPR spectra of **3** in dmso solution at 90 K when the concentration is changed.

Tentatively, we suggest that the formation of a dinuclear species from two $[CuL(py)_2]$ molecules might occur by attack of the O(6) exocyclic atom of the pyrimidine ring of each $[CuL(py)_2]$ molecule on the copper atom of the neighbouring one, with either subsequent or simultaneous elimination of two molecules of pyridine, one from each mononuclear entity. This process would facilitate the generation of an oxygen-bridged dinuclear complex. We have already observed this type of structure for the dinuclear complex $[\{CuL(Him)\}_2]$.[14]

Acknowledgements

We are grateful to the Dirección General de Investigación Científica y Técnica for the project of investigation PB88-0482 and to the Junta of Andalucia for financial support, as well as to

Dr. J. Parry for reviewing the manuscript. J. M. M. and J. M. D.-V. are grateful to the Ministry of Education and Science for a grant. M. R. S. thanks Emil Aaltonen Foundation for a grant.

References

1 M. Inoue and M. Kubo, *Inorg. Chem.*, 1970, **9**, 2310.
2 G. Kolks, S. J. Lippard and J. V. Waszczack, *J. Am. Chem. Soc.*, 1980, **102**, 4832.
3 P. J. Corvan, W. E. Estes, R. R. Weller and W. E. Hatfield, *Inorg. Chem.*, 1980, **19**, 1297.
4 D. K. Towle, S. K. Hoffmann, W. E. Hatfield, P. Singh and P. Chaudhuri, *Inorg. Chem.*, 1988, **27**, 349.
5 P. K. Coughlin and S. J. Lippard, *J. Am. Chem. Soc.*, 1984, **106**, 2328.
6 R. L. Carlin, K. Kopinga, O. Khan and M. Verdaguer, *Inorg. Chem.*, 1986, **25**, 1786.
7 A. Fuertes, C. Miratvilles, E. Escriva, E. Coronado and E. Beltran, *J. Chem. Soc., Dalton Trans.*, 1986, 1975.
8 E. Colacio, J. P. Costes, R. Kivekäs, J. P. Laurent and J. Ruiz, *Inorg. Chem.*, 1990, **29**, 4240.
9 E. Colacio, J. M. Dominguez-Vera, J. P. Costes, R. Kivekäs, J. P. Laurent, J. Ruiz and M. Sundberg, *Inorg. Chem.*, 1992, **31**, 774.
10 M. S. Masoud, S. A. Abou Ali, G. Y. Ali and I. M. Abed, *Thermochim. Acta*, 1987, **122**, 209.
11 G. M. Sheldrick, SHELXS 86, Program for Solution of Crystal Structure, University of Göttingen, 1986.
12 S. R. Hall and J. M. Stewart (Editors), XTAL 3.0 for IBM PCs and Compatibles, Adapted for MS(PC)-DOS computers by D. A. Grossie, Wright State University, Reference Manual, Universities of Western Australia and Maryland, 1990.
13 SHELXTL-PLUS program, X-Ray Instruments Group, Nicolet Instrument Corporation, Madison, WI, 1990.
14 J. M. Dominguez-Vera, J. Ruiz, M. Sundberg, R. Kivekäs, J. M. Moreno and E. Colacio, unpublished work.
15 E. L. Muetterties and L. J. Guggenberg, *J. Am. Chem. Soc.*, 1974, **96**, 1748.
16 A. W. Addison, P. J. Burke and K. Henrick, *Inorg. Chem.*, 1982, **21**, 60.
17 B. J. Hathaway and A. A. Tomlinson, *Coord. Chem. Rev.*, 1970, **5**, 1; B. J. Hathaway and D. E. Billing, *Coord. Chem. Rev.*, 1970, **5**, 143; B. J. Hathaway, *Struct. Bonding (Berlin)*, 1984, **57**, 55.
18 A. Bencini and D. Gatteschi, *EPR of Exchange Coupled Systems*, Springer, Heidelberg, 1990.
19 F. Nepveu, *Inorg. Chim. Acta*, 1987, **134**, 43 and refs. therein.
20 T. D. Black, R. S. Rubins, D. K. De, R. C. Dickinson and W. A. Baker, *J. Chem. Phys.*, 1984, **80**, 4620.
21 A. Bencini, D. Gattechi, C. Zanchini, J. G. Haasnoot, R. Prins and J. Reedijk, *J. Am. Chem. Soc.*, 1987, **109**, 2926.
22 R. Prins, R. A. G. de Graaff, J. G. Haasnoot, C. Vader and J. Reedijk, *J. Chem. Soc., Chem. Commun.*, 1986, 1430 and refs. therein.
23 R. W. Jotham and S. F. A. Kettle, *Inorg. Chim. Acta*, 1970, **4**, 145.
24 R. Mergehenn, L. Merz and W. Haase, *J. Chem. Soc., Dalton Trans.*, 1980, 1703.
25 G. A. Baker, G. S. Rushbrooke and H. E. Gilbert, *Phys. Rev. A*, 1964, **135**, 1272.
26 O. Khan, *Magneto-Structural Correlations in Exchange Coupled Systems*, eds. R. D. Willett, D. Gatteschi and O. Khan, D. Reidel, Dordrecht, 1985.
27 C. J. O'Connor, *Prog. Inorg. Chem.*, 1982, **29**, 203.
28 T. R. Felthouse and D. N. Hendrickson, *Inorg. Chem.*, 1978, **17**, 444.

Received 2nd *June* 1992; *Paper* 2/02894H